

Optimizing Laccase Production in Auricularia Cornea by Submerged Fermentation With Wheat Bran Extract: Applications in Decolorization of Malachite Green Dye

Li Meng

Shandong Agricultural University

Xiaoran Bai (✉ bxr777@126.com)

Shandong Agricultural University <https://orcid.org/0000-0002-9145-7748>

Qingji Wang

Shandong Agricultural University

Xiaobo Li

Shandong mushroom industrial technology innovation research institute

Shaoyan Zhang

Shandong Agricultural University

Li Wang

Shandong Agricultural University

Wei Wang

Shandong Agricultural University

Zhuang Li

Shandong Agricultural University

Original article

Keywords: Wood ear mushroom, Laccase, Decolorization, Biodegradation

Posted Date: April 29th, 2021

DOI: <https://doi.org/10.21203/rs.3.rs-464777/v1>

License:  This work is licensed under a Creative Commons Attribution 4.0 International License.

[Read Full License](#)

1

2 **Optimizing laccase production in *Auricularia cornea* by submerged fermentation with**
3 **wheat bran extract: Applications in decolorization of malachite green dye**

4

5 Li Meng^{a, #}, Xiao-ran Bai^{a, #}, Qing-ji Wang^a, Xiao-bo Li^b, Shao-yan Zhang^a, Li Wang^a,

6 Wei Wang^a, Zhuang Li^{a, *}

7 ^a Shandong Provincial Key Laboratory of Agricultural Microbiology, College of Plant

8 Protection, Shandong Agricultural University, Tai'an 271018, China

9 ^b Shandong Mushroom Industrial Technology Innovation Research Institute, Jining,

10 272000, China

11 [#]The authors contributed equally to this work.

12 ^{*}Corresponding author: liz552@126.com

13 **Abstract:**

14 Wheat bran extract may enhance laccase activity of *Auricularia cornea* in submerged
15 fermentation. The laccase activity of *A. cornea* was maximal (768.78 U/mL) at 26.9 °C, pH 5,
16 a time point of 6 d, 22 h, and an inducer concentration of 10%. Laccase from *A. cornea* AC5
17 decolorized 83.27% of 75 mg/L malachite green within 12 h. High performance liquid
18 chromatography (HPLC) analysis of the extracted metabolites suggested that the
19 decolorization occurred through biodegradation. Malachite green induced cytotoxic damage
20 including formation of a micronucleus and chromosome bridge at anaphase. Degradation
21 products of malachite green proved to be less toxic and had negligible effects on
22 chromosomal aberrations.

23 **Key words:**

24 Wood ear mushroom, Laccase, Decolorization, Biodegradation

25 **Introduction**

26 Robust growth of the worldwide textile industry in recent years has driven a
27 commensurate increase in the use of synthetic dyes and consequent environmental pollution
28 due to the discharge of contaminated wastewater (Saratale et al. 2011). Triphenylmethane
29 dyes, including malachite green, are among the most widely used group of synthetic colorants
30 for dyeing cotton, wool, silk, nylon, etc. (Ayed et al. 2009). However, malachite green is
31 highly toxic to mammalian cells. It promotes hepatic tumor formation in rodents and causes
32 reproductive abnormalities in rabbits and fish (Fernandes et al. 1991; Rao 1995). Moreover,
33 removal of dye chemicals from dye-bearing wastewater is a complex problem because of
34 difficulty in wastewater treatment using conventional methods (Kumar et al. 2006), such as,
35 ozonation, photooxidation, electrocoagulation, adsorption, reverse osmosis, membrane
36 filtration, etc. (Daneshvar et al. 2007; Jain et al. 2003). Therefore, developing a new, practical
37 method for their removal from wastewater is of utmost importance (Ayed et al. 2011).

38 *Auricularia cornea* is a type of white-rot fungus which has been intensively studied for
39 its dye-decolorizing properties. Non-specific lignin-modifying enzymes in white-rot fungi
40 enable them to transform a wide range of organic compounds (Wesenberg et al. 2003). There
41 are a considerable number of recent studies on decolorization and degradation of individual
42 synthetic dyes including triphenylmethane (Viřanská et al. 2018), azo (Tauber et al. 2005),
43 anthraquinone (Tychanowicz et al. 2004), etc. by white-rot fungi (Asgher et al. 2006). The
44 biodegradation ability of white-rot fungi is assumed to be associated with the production of
45 lignolytic enzymes such as lignin peroxidase and laccase (Couto and Herrera 2006; Ghodake
46 et al. 2008). In addition, most studies have found that fungi with the highest laccase activity,

47 for instance, *Trametes versicolor* (Li et al. 2014), *Fomes fomentarius* (Neifar et al. 2011),
48 *Ganoderma* sp. (Zhuo et al. 2011), *Agaricus bisporus* (Othman et al. 2018), *Thelephora* sp.
49 (Selvam K et al. 2003), and *Pleurotus* sp. (Tychanowicz et al. 2004; Meng and Li 2017) can
50 decolorize dyes the most efficiently (Erkurt et al. 2007). This suggests that laccase plays a key
51 role in this process.

52 Laccase (EC 1.10.3.2, benzenediol/oxygen oxidoreductase) is a multicopper oxidase,
53 widely distributed among plants, fungi, and bacteria (Claus 2003). When different sources of
54 laccase catalyze the same substrate, the enzymatic characteristics are different. When the
55 same laccase catalyzes different substrates, the enzymatic characteristics are also different. In
56 order to better apply the use of laccase for remediation, optimization of cultivation conditions
57 is an important strategy to maximize laccase enzyme productivity (Bhattacharya et al. 2011).
58 Some researchers have reported increases in laccase activity following the addition of
59 different inducers to media, such as veratryl alcohol, Tween-80, copper sulphate or
60 2,5-xylydine (Churapa et al. 2007; Sondhi and Saini 2019; Galhaup and Haltrich 2001). In
61 addition, many studies have shown that the nitrogen (N) source, as one of the important
62 nutritional factors in fungal metabolism, can regulate the production of ligninolytic enzymes
63 in wood-rotting basidiomycetes (Galhaup et al. 2002; Sun et al. 2004). Laccase production by
64 *Trametes modesta* can be significantly influenced by wheat bran, yeast extract and incubation
65 temperature (Nyanhongo et al. 2002). The laccase activity of *Ganoderma lucidum* 447 was
66 the highest in submerged fermentation processes using wheat or soybean bran (Songulashvili
67 et al. 2007), with evidence that enzyme activity was influenced the N source.

68 This study aims to investigate the potential of *A. cornea* for decolorizing a solution

69 containing a cationic textile dye, malachite green. Correlation of laccase activity with various
70 parameters (time, temperature, inducer concentration and pH) were characterized. The
71 cytogenotoxicity of the products formed after decolorization were studied.

72 **Materials and methods**

73 **Organisms and preparation of crude enzyme solution**

74 An *A. cornea* AC5 strain was provided by the Collection Center of Mushrooms in Jilin
75 Agricultural University. The strain was maintained on potato dextrose agar (PDA) medium at
76 18 °C. Five 0.7-cm potato dextrose agar discs of mycelia from a Petri dish were inoculated in
77 a flask with 100 mL complete yeast medium (CYM) (1% maltose, 2% glucose, 0.2% yeast
78 extract, 0.2% tryptone, 0.05% MgSO₄·7H₂O, 0.46% KH₂PO₄), followed by shaking the
79 culture at 26°C and 160r/min. After seven days, the cultures were centrifuged at 6000r/min
80 for 10min, and the cell-free supernatant was used as a crude enzyme solution.

81 **Effects of different physicochemical parameters on laccase activity**

82 To obtain a representative picture of laccase activity, preliminary experiments were
83 conducted at different temperatures (22-34 °C) at pH 5, at various other pH ranges (3-9) at
84 26 °C, as well as at pH 5, at different inducer concentrations (0-20%) at 26 °C and pH 5, and
85 with different cultivation periods (1-9 d) at 26 °C and pH 5. The factors affecting the laccase
86 production of *A. cornea* AC5 were screened on the basis of these preliminary experiments.
87 The effects of these parameters on laccase activity were examined by varying only one factor at a
88 time, where time, temperature, inducer concentration and pH were considered as key variables.
89 All of these experiments were performed under aseptic conditions under isothermal
90 incubation at a constant agitation of 160 rpm in a 250 mL Erlenmeyer flask with a 5% inducer

91 concentration (except experiments measuring the effects of different inducer concentrations).

92 **Laccase activity assay**

93 Laccase activity was determined by monitoring the A_{420} change related to the rate of
94 oxidation of 1 μmol of 2,2-azino-bis-[3-ethylthiazoline-6-sulfonate] (ABTS) in 20 mM of a
95 sodium acetate buffer (pH 4.5). Assays were performed in a 1 mL spectrophotometric cuvette
96 at 30 °C with an adequately diluted culture liquid. One unit of laccase activity was defined as
97 the amount of enzyme catalyzing the oxidation of 1 μmol of ABTS per minute.

98 **Selection of significant parameters by Plackett-Burman (PB)**

99 A set of 27 experiments was designed using the Plackett-Burman design of Design
100 Expert (version 8.0.6.1) software for four variables (Table 1, 2) that were analyzed as possible
101 factors affecting production. The parameters evaluated were as follows: A: time, B:
102 temperature, C: inducer concentration, D: pH. Ideal concentration levels were calculated based on
103 single factor analysis. All the trials were carried out in triplicate and the mean laccase yield was
104 calculated.

105 **Optimization of laccase production using response surface methodology (RSM)**

106 Central composite design (CCD) of RSM in Design Expert (version 8.0.6.1) was
107 employed at an α value of ± 1 to further optimize the levels of significant variables (Table 1).
108 Laccase activity was recorded as the response. Response data were analyzed by the software
109 to generate 3D plots indicating the optimum conditions and interactions among these factors.
110 A regression analysis was performed on the data obtained. A second-order polynomial
111 equation was used to fit the data by a multiple regression procedure. A quadratic model was
112 obtained as per the following equation:

113
$$Y = \delta_0 + \sum \delta_i V_i + \sum \delta_{ii} V_{i2} + \sum \delta_{ij} V_i V_j$$

114 Where, Y is the predicted response [laccase activity (U/mL)], δ_0 is the constant term, δ_i
115 the linear coefficients, δ_{ii} the squared coefficients and δ_{ij} the interaction coefficients. The
116 quality of fit by the polynomial model equation was expressed using the coefficient of
117 determination, R^2 .

118 **Analytical methods in dye decolorization**

119 Dye colors were determined spectrophotometrically (Abadulla et al. 2000). Color
120 removal was determined based on absorbance in the UV-visible spectrum using a previously
121 described equation (Jadhav et al. 2008). The decolorization rate (%) was calculated as $(A_i - A_t)$
122 $/ A_i \times 100$, where A_i and A_t are the initial and final absorbance units, respectively.

123 The decolorization of malachite green dye was determined by High Performance Liquid
124 Chromatography (HPLC). Chromatographic separation of samples was performed using an
125 Eclipse Plus 95Å C18 column (4.5 × 250mm, 5 µm). The column temperature was maintained
126 at 30 °C. Mobile phase A was 0.125 mol/mL ammonium acetate solution and mobile phase B
127 was acetonitrile. The elution profile was set as following: 0.01 min, 80% B; 20min, 80% B.
128 The flow rate was 1.00 mL/min, the injection volume was 20 µL and absorbance was
129 measured at 614 nm.

130 **Cytogenotoxicity test**

131 *Allium sativum* was used to study the cytotoxicity of malachite green. The meristematic
132 cells of root tips were exposed to malachite green dye for 24 h. These root tips were later
133 fixed in Carnoy's Fluid for 3h. Fixation was followed with treatment with 1 M HCl at 60 °C
134 for 8 min, followed by a distilled water rinse. Root tips were squashed on a glass slide in

135 Schiff reagent for 10 min. The prepared slide samples were sealed with a coverslip and
136 observed at 400× and 1000× magnification.

137 **Results**

138 **Determination of optimum time, temperature, inducer concentration and pH for laccase** 139 **activity**

140 Adaptation of the fungus to a broader range in pH and temperature may improve its
141 suitability for laccase production. [Figure 1C](#) shows that laccase activity was maximal (625.14
142 U/mL) at 7.5% inducer concentration. The laccase activity was 386.61 U/mL, 321 U/mL and
143 346.94 U/mL at 9 d, 26 °C and pH 5, respectively ([Figure 1A, B, D](#)). The laccase activity of *A.*
144 *cornea* increased proportionally with culture time. However, the liquid medium became
145 considerably more viscous by the 9th day. Therefore, we focused on laccase activity at 3-7 d
146 for further study.

147 **Optimization of laccase activity of *A. cornea* AC5 using CCD by RSM approach**

148 The experiments were conducted as per the combination listed in [Table 2](#). Multiple
149 regression analysis was carried out and fitted to a second degree polynomial equation, which
150 relates dependent and independent variables, as indicated:

$$\begin{aligned} 151 \quad R1 = & 576.47983 + 33.275152779167A + 156.64087497083B - 69.960944458333C - 115.6875 \\ 152 \quad & 0001667D + 101.702166625AB - 11.748708375AC + 35.5289166625AD - 21.723541675BC - 11 \\ 153 \quad & 8.0526667125BD - 175.587916675CD - 171.30556249792A^2 - 143.77193753542B^2 - 16.914166 \\ 154 \quad & 679167 C^2 - 113.57749997917D^2 \end{aligned}$$

155 The fitness of the quadratic polynomial equation generated was statistically verified by
156 an F-test (ANOVA). [Table 3](#) shows the analysis of variance (ANOVA) for the generated

157 model for the process, with a significance level of $p < 0.05$. An R^2 value of 99.93% measured
158 for laccase production indicated a good fit for the generated model. The "Lack of Fit" p -value
159 of 0.0706 (non-significant) supported this inference. The variations in responses as a function
160 of the assessed parameters are represented in a 3D response surface plot as shown in [Figure 2](#).
161 A response surface contour map directly reflects the influence of various factors on the value
162 of a specific response, so as to determine the best process parameters and their interactions.
163 The higher the slope of the surface, the steeper the slope, indicating that a significant
164 interaction beyond a certain degree of slope. In addition, laccase activity decreased gradually
165 when the color of the surface changed from red to green. The center of the smallest ellipse of
166 the contour on the surface was the highest point of the response surface, corresponding to
167 maximal enzyme activity. The model forecasted that peak laccase production of *A. cornea*
168 was 787.87 U/mL at 26.9 °C and pH 5, with an incubation time of 6d, 22 h, and an inducer
169 concentration of 10%. The optimal extraction conditions were verified experimentally, and
170 the results indicated that the laccase yield was 768.78 U/mL, which was consistent with the
171 model.

172 **Decolorization of malachite green dye**

173 Laccase from *A. cornea* AC5 decolorized 83.27% of malachite green at an initial
174 concentration of 75 mg/L within 12 h. High performance liquid chromatography (HPLC)
175 analysis results revealed that the peak elution time of malachite green was at 2.373 min, the
176 peak height was 696.445 mAU and the peak area was 34.595 mAU*min ([Figure 3 A](#)).
177 Degraded malachite green dye was also detected by HPLC, with a peak height of 16.479
178 mAu at an elution time of 1.997 min; the peak area was 0.653 mAu *min ([Figure 3 B](#)). HPLC

179 analysis of the extracted metabolites suggested that the decolorization occurred through
180 biodegradation.

181 **Cytogenotoxicity**

182 Malachite green dye is known to generate carcinogenic compounds after breakdown in
183 some instances. *Allium sativum* is a well-accepted and reliable model for testing
184 cytogenotoxic effects. As demonstrated in [Figure 4](#), malachite green treatment was associated
185 with an increase in chromosomal aberrations. Malachite green induced cytotoxic damage
186 including micronucleus ([Figure 4A](#)) and chromosome bridge at anaphase ([Figure 4B](#)). The
187 degradation products of malachite green after treatment with *A. cornea* AC5 were
188 considerably less cytogenotoxic and had a negligible effect on induced chromosomal
189 aberrations.

190 **Discussion**

191 In this study, we found that wheat bran extract significantly enhanced the laccase activity
192 of *A. cornea* in submerged fermentation. This result was consistent with that wheat bran could
193 improve the bacterial laccase activity ([Muthukumarasamy et al. 2015](#)). The concentration of
194 wheat bran extract was directly correlated to the production of laccase up to a concentration
195 of 7.5%. Above this concentration, laccase production was inversely correlated to the
196 concentration of wheat bran extract. This suggests that the presence of wheat bran extract
197 increased the amount of N in the liquid media ([Bagewadi et al. 2017](#)). Above a certain point,
198 an excess N:C ratio increases the viscosity of the fermentation broth, which is not conducive
199 to the growth of mycelia.

200 Laccases can efficiently degrade different types of dyes ([Legerská et al. 2016](#)), for

201 instance, triphenylmethane, anthraquinone, thiazine, azo, etc. In this study, we found that
202 laccase from *A. cornea* AC5 degraded the triphenylmethane dye, malachite green. The
203 decolorization rate of malachite green (75 mg/L) was 83.27% within 12 h. To understand the
204 bioremediation mechanisms involved, we predict the propensity of redox enzymes to degrade
205 dyes, based on bioinformatics research and molecular modeling docking tools (Lohning et al.
206 2017). We obtained a laccase protein sequence in *A. cornea* by Protein BLAST. The PDB
207 Format laccase and Mol2 Format small dye molecules were simulated by AutoDock software
208 (Figure 5), and a minimum binding energy of -28.37 kJ/mol was obtained, which was plotted
209 by PyMoL and LigPlus for analysis. It is generally accepted that an energy well occurs when
210 a stable conformation of the ligand and its receptor binding is present (Lin et al. 2020). With a
211 value of binding energy lower than -5 kJ/mol, the better the binding effect, and the greater the
212 possibility of action. The laccase-dye complex was tested in vitro to verify the effectiveness
213 of dye bioremediation. The results indicated that the combination of laccase structure
214 prediction via modeling and in vitro analysis is an effective preliminary screening method,
215 which can be further applied to the real-time treatment of toxic wastewater in the textile
216 industry.

217 **Declarations**

218 **Ethical approval Not applicable** Not applicable

219 **Consent to participate** All the authors agree to participate.

220 **Consent to publish** We consent to publish this manuscript in the Environmental Science and
221 Pollution Research. This manuscript has not been published in whole or in part nor is it being
222 considered for publication elsewhere.

223 **Availability of data and materials** All data generated or analyzed during this study are
224 included in this manuscript.

225 **Competing interests** The authors declare no competing interests.

226 **Funding** This work was financially supported by National Key Research and Development
227 Program of China [grant number 2018YFD1001001].

228 **Authors' contribution** Conceived and designed the experiments: LM, LW, WW. Performed
229 the experiments: XRB and SYZ. Analyzed the data: QJW and XRB. Wrote the paper: LM and
230 XRB. Editing and supervision: ZL and XBL. All authors read and approved the final
231 manuscript.

232 **Acknowledgements** The authors would like to thank to all who contributed to this study.

233 **References**

234 Abadulla E, Tzanov T, Costa S, Robra KH, Cavaco-Paulo A, Gubitz GM (2000)
235 Decolorization and detoxification of textile dyes with a laccase from *Trametes hirsuta*.
236 *Applied and Environmental Microbiology* 66: 3357.

237 Asgher M, Shah SAH, Ali M, Legge RL (2006) Decolorization of some reactive dyes by
238 white rot fungi isolated in Pakistan. *World Journal of Microbiology Biotechnology* 22:
239 89-93.

240 Ayed L, Chaieb K, Cheref A, Bakhrouf A (2009) Biodegradation of triphenylmethane dye
241 malachite green by *Sphingomonas paucimobilis*. *World J Microbiol Biotechnol* 25:
242 705-711.

243 Ayed L, Mahdhi A, Cheref A, Bakhrouf A (2011) Decolorization and degradation of azo dye
244 Methyl Red by an isolated *Sphingomonas paucimobilis*: Biotoxicity and metabolites

245 characterization. *Desalination* 274: 272-277.

246 Bagewadi ZK, Mulla SI, Ninnekar HZ (2017) Optimization of laccase production and its
247 application in delignification of biomass. *International Journal of Recycling of Organic*
248 *Waste in Agriculture* 6: 351-365.

249 Bhattacharya SS, Garlapati VK, Banerjee R (2011) Optimization of laccase production using
250 response surface methodology coupled with differential evolution. *New Biotechnol* 28:
251 31-39.

252 Teerapatsakul C, Parra R, Bucke C, Chitradon L (2007) Improvement of laccase production
253 from *Ganoderma* sp. KU-Alk4 by medium engineering. *World Journal of Microbiology*
254 *& Biotechnology* 23: 1519-1527.

255 Claus H (2003) Laccase and their occurrence in prokaryotes. *Achieve in Microbiology* 179:
256 145-150.

257 Couto RS, Herrera JTL (2006) Industrial biotechnological applications of laccases: A review.
258 *Biotechnology Advance* 24: 500-513.

259 Daneshvar N, Khataee AR, Rasoulifard MH, Pourhassan M (2007) Biodegradation of dye
260 solution containing Malachite Green: optimization of effective parameters using Taguchi
261 method. *J Hazard Mater* 143: 214-219.

262 Erkurt EA, Ali ü, Kumbur H (2007) Decolorization of synthetic dyes by white rot fungi,
263 involving laccase enzyme in the process. *Process Biochemistry* 42: 1429-1435.

264 Fernandes C, Lalitha VS, Rao KVK (1991) Enhancing effect of Malachite Green on the
265 development of hepatic pre-neoplastic lesions induced by N-nitrosodiethylamine in rats.
266 *Carcinogenesis* 12: 839-845.

267 Galhaup C, Haltrich D (2001) Enhanced formation of laccase activity by the white rot fungus
268 *Trametes pubescens* in the presence of copper. *Appl Microbiol Biotechnol* 56: 225-232.

269 Galhaup C, Wagner H, Hinterstoisser B, Haltrich D (2002) Increased production of laccase by
270 the wood-degrading basidiomycete *Trametes pubescens*. *Enzyme Microb Technol* 30:
271 529-536.

272 Ghodake GS, Kalme SD, Jadhav JP, Govindwar SP (2008) Purification and partial
273 characterization of lignin peroxidase from *Acinetobacter calcoaceticus* NCIM 2890 and
274 its application in decolorization of textile dyes. *Applied Biochemistry and Biotechnology*
275 152: 6-14.

276 Jadhav UU, Dawkar VV, Ghodake GS, Govindwar SP (2008) Biodegradation of Direct Red
277 5B, a textile dye by newly isolated *Comamonas* sp. UVS. *Journal of Hazardous*
278 *Materials* 158: 507-516.

279 Jain IA, Gupta VK, Bhatnagar-Suhas A (2003) Utilization of industrial waste products as
280 adsorbents for the removal of dyes. *J Hazard Mater B* 101: 31-42.

281 Kumar KV, Ramamurthi V, Sivanesan S (2006) Biosorption of malachite a green, a cationic
282 dye onto *Pithophora* sp., a fresh water algae. *Dyes Pigments* 69: 74-79.

283 Legerská B, Chmelová D, Ondrejovič M (2016) Degradation of synthetic dyes by laccases.
284 *Nova Biotechnologica et Chimica* 15: 90-106.

285 Li A, Ge L, Cai J, Pei J, Xie J, Zhao L (2014) Comparison of Two Laccases from *Trametes*
286 *versicolor* for Application in the Decolorization of Dyes. *J Microbiol Biotechnol* 24(4):
287 545-555.

288 Lin Z, Tong Y, Li N, Zhu Z, Li J (2020) Network pharmacology-based study of the

289 mechanisms of action of anti-diabetic triterpenoids from *Cyclocarya paliurus*. Royal
290 society of chemistry advances 10: 37168. <https://doi.org/10.1039/D0RA06846B>

291 Lohning AE, Levonis SM, Williams-Noonan B, Schweiker SS (2017) A practical guide to
292 molecular docking and homology modelling for medicinal chemists. Current Topics in
293 Medicinal Chemistry 17: 1-18.

294 Meng L, Li Y (2017) Evaluation of the capacity to decolorize synthetic dyes by the wild strain
295 JY2746 of *Pleurotus ostreatus*. Mycosystema 36(11): 1575-1582.

296 Muthukumarasamy NP, Jackson B, Raj AJ, Sevanan M (2015) Production of extracellular
297 laccase from *Bacillus subtilis* MTCC 2414 using agroresidues as a potential substrate.
298 Biochemistry research international ID 765190.

299 Neifar M, Jaouani A, Kamoun A, Ellouze-Ghorbel R, Ellouze-Chaabouni S (2011)
300 Decolorization of Solophenyl Red 3BL Polyazo Dye by Laccase-Mediator System:
301 Optimization through Response Surface Methodology. Enzyme Res 179050.
302 <https://doi.org/10.4061/2011/179050>

303 Nyanhongo GS, Gomes J, Gübitz G, Zvauya R, Read JS, Steiner W (2002) Production of
304 laccase by a newly isolated strain of *Trametes modesta*. Bioresource Technology 84:
305 259-263.

306 Othman AM, Elsayed MA, Elshafei AM, Hassan MM (2018) Application of central
307 composite design as a strategy to maximize the productivity of *Agaricus bisporus* cu13
308 laccase and its application in dye decolorization. Biocatalysis and Agricultural
309 Biotechnology 14: 72-79.

310 Rao KVK (1995) Inhibition of DNA synthesis in primary rat hepatocyte cultures by Malachite

311 Green: a new liver tumor promoter. *Toxicol Lett* 81: 107-113.

312 Saratale RG, Saratale GD, Chang JS, Govindwar SP (2011) Bacterial decolorization and
313 degradation of azo dyes: A review. *J Taiwan Inst Chem Eng* 42, 138-157.

314 Selvam K, Swaminathan K, Chae KS (2003) Decolourization of azo dyes and a dye industry
315 effluent by a white rot fungus *Thelephora* sp.. *Bioresour Technol* 88:115-119.

316 Sondhi S, Saini K (2019) Response surface based optimization of laccase production from
317 *Bacillus* sp. MSK-01 using fruit juice waste as an effective substrate. *Heliyon* 5: e01718.

318 Songulashvili G, Elisashvili V, Wasser SP, Nevo E, Hadar Y, Basidiomycetes laccase and
319 manganese peroxidase activity in submerged fermentation of food industry wastes,
320 *Enzyme Microb Technol* 41: 57-61.

321 Sun X, Zhang R, Zhang Y (2004) Production of lignocellulolytic enzymes by *Trametes*
322 *gallica* and detection of polysaccharide hydrolase and laccase activities in
323 polyacrylamide gels. *J Basic Microbiol* 44: 220-231.

324 Tauber MM, Guebitz GM, Rehorek A (2005) Degradation of Azo Dyes by Laccase and
325 Ultrasound Treatment. *Applied and Environmental Microbiology* 71(5): 2600-2607.

326 Tychanowicz GK, Zilly A, de Souza CGM, Peralta RM (2004) Decolourisation of industrial
327 dyes by solid-state cultures of *Pleurotus pulmonarius*. *Process Biochemistry* 39(7):
328 855-859.

329 Vršanská M, Voběrková S, Jiménez AMJ, Strmiska V, Adam V (2018) Preparation and
330 Optimisation of Cross-Linked Enzyme Aggregates Using Native Isolate White Rot Fungi
331 *Trametes versicolor* and *Fomes fomentarius* for the Decolourisation of Synthetic Dyes.
332 *International Journal of Environmental Research and Public Health* 15: 23.

333 <https://doi.org/10.3390/ijerph15010023>

334 Wesenberg D, Kyriakides I, Agathos SN (2003) White-rot fungi and their enzymes for the
335 treatment of industrial dye effluents. *Biotechnology Advances* 22: 161-187.

336 Zhuo R, Ma L, Fan FF, Gong YM, Wan X, Jiang ML, Zhang XY, Yang Y (2011)
337 Decolorization of different dyes by a newly isolated white-rot fungi strain *Ganoderma* sp.
338 En3 and cloning and functional analysis of its laccase gene. *Journal of Hazardous*
339 *Materials* 192: 855-873.

340

341 **Figure Captions**

342 Figure 1 Effects of time (A), temperature (B), inducer concentration (C) and pH (D) on the
343 laccase activity of *Auricularia cornea*.

344 Figure 2 The influence of the interactions of two combinations of factors on laccase
345 production in *Auricularia cornea*. (A) Interaction between inducer concentration and pH.
346 (B) Interaction between inducer concentration and time. (C) Interaction between inducer
347 concentration and temperature. (D) Interaction between temperature and time.

348 Figure 3 Decolorization analysis of malachite green dye by HPLC. (A) Original sample of
349 malachite green dye. (B) Malachite green after degradation by *A. cornea* AC5 for 12 h.

350 Figure 4 Cytotoxic damage induced in root meristematic cells of *Allium sativum* on treatment
351 with malachite green. The black arrow in the picture refers to the chromosome variant
352 cells. (A) micronucleus, (B) chromosome bridge.

353 Figure 5 Structural model of molecular docking complex. (A) 3D model of molecular docking
354 complex of laccase from *A. cornea* AC5 and Malachite green. (B) 2D ligand-receptor
355 interaction diagram. Ligand interaction diagram indicating in detail how these residues
356 interact with the ligand. Note the interactions between amino groups and acidic residues,
357 specifically at Asn82, Ser135, Glu175, Ala537, Asp539, Phe536, and Asp178.

358

Table 1 Factors and coded levels of the central composite design

Factors	Code	Level		
		-1	0	1
Time (d)	A	3	5	7
Temperature (°C)	B	22	26	30
Inducer concentration (%)	C	5	7.5	10
pH	D	5	6	7

Table 2 Experimental design and results of preliminary experiments on laccase activity in

Auricularia cornea

Run No.	Factors				Laccase activity (U/mL)
	A: Time (h)	B: Temperature (°C)	C: Inducer concentration (%)	D: pH	
1	0	-1	0	1	61.91
2	-1	0	0	1	282.59
3	-1	0	1	0	205.56
4	1	-1	0	0	302.23
5	0	1	0	1	218.62
6	0	-1	1	0	310.66
7	0	0	-1	-1	466.35
8	-1	0	-1	0	220.78
9	-1	-1	0	0	118.98
10	0	-1	0	-1	404.03
11	0	0	1	-1	654.33
12	-1	1	0	0	0.62
13	0	0	0	0	593.35
14	-1	0	0	-1	224.28
15	1	1	0	0	590.67
16	0	1	0	-1	418.63
17	0	1	-1	0	537.51
18	0	0	0	0	580.91
19	0	-1	-1	0	485.06
20	0	0	-1	1	572.27
21	1	0	1	0	535.76
22	1	0	0	1	226.03
23	1	0	-1	0	637.88
24	0	0	0	0	555.19
25	1	0	0	-1	639.93
26	0	0	1	1	57.90
27	0	1	1	0	316.11

Table 3 Regression variance results of the experimental model

Sources	Sum of squares	Df	Sum of squares	F value	P value	Significant
Model	995899.3315	14	71135.66653	16.37894561	< 0.0001	significant
A-A	13286.82951	1	13286.82951	3.059284722	0.1058	
B-B	294436.3645	1	294436.3645	67.79380069	< 0.0001	
C-C	58734.40499	1	58734.40499	13.52356239	0.0032	
D-D	160603.1719	1	160603.1719	36.97878638	< 0.0001	
AB	41373.32278	1	41373.32278	9.526183368	0.0094	
AC	552.1285939	1	552.1285939	0.127127286	0.7276	
AD	5049.215677	1	5049.215677	1.162578956	0.3021	
BC	1887.649052	1	1887.649052	0.43463009	0.5222	
BD	55745.72847	1	55745.72847	12.83542137	0.0038	
CD	123324.4659	1	123324.4659	28.39538614	0.0002	
A ²	156509.844	1	156509.844	36.03630002	< 0.0001	
B ²	110241.9735	1	110241.9735	25.3831499	0.0003	
C ²	1525.808184	1	1525.808184	0.351316442	0.5644	
D ²	68799.19201	1	68799.19201	15.84097371	0.0018	
Residual	52117.39626	12	4343.116355			
Lack of fit	51359.82189	10	5135.982189	13.55901791	0.0706	not significant
Pure error	757.5743644	2	378.7871822			
Cor total	1048016.728	26				

Figures

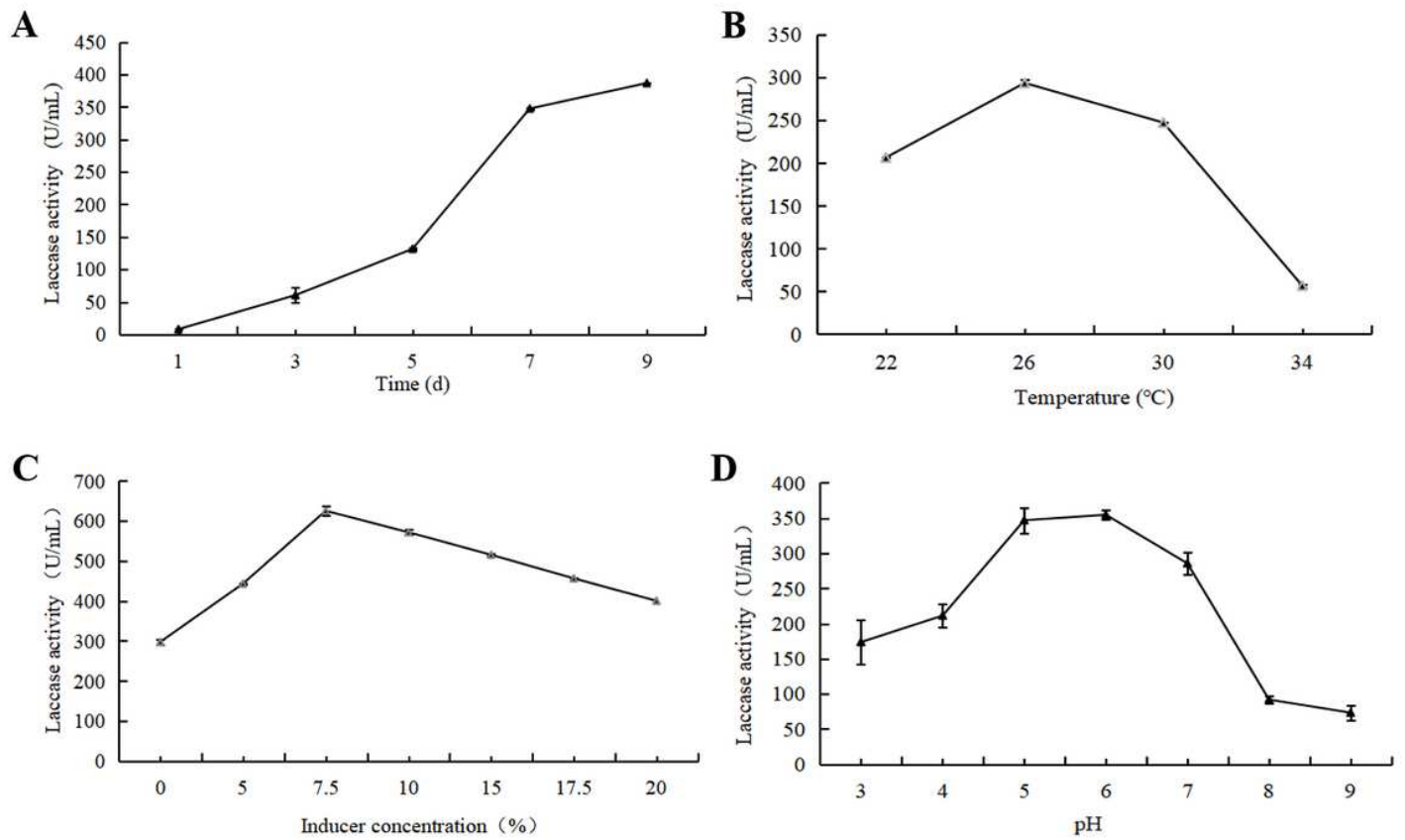


Figure 1

Effects of time (A), temperature (B), inducer concentration (C) and pH (D) on the laccase activity of *Auricularia cornea*.

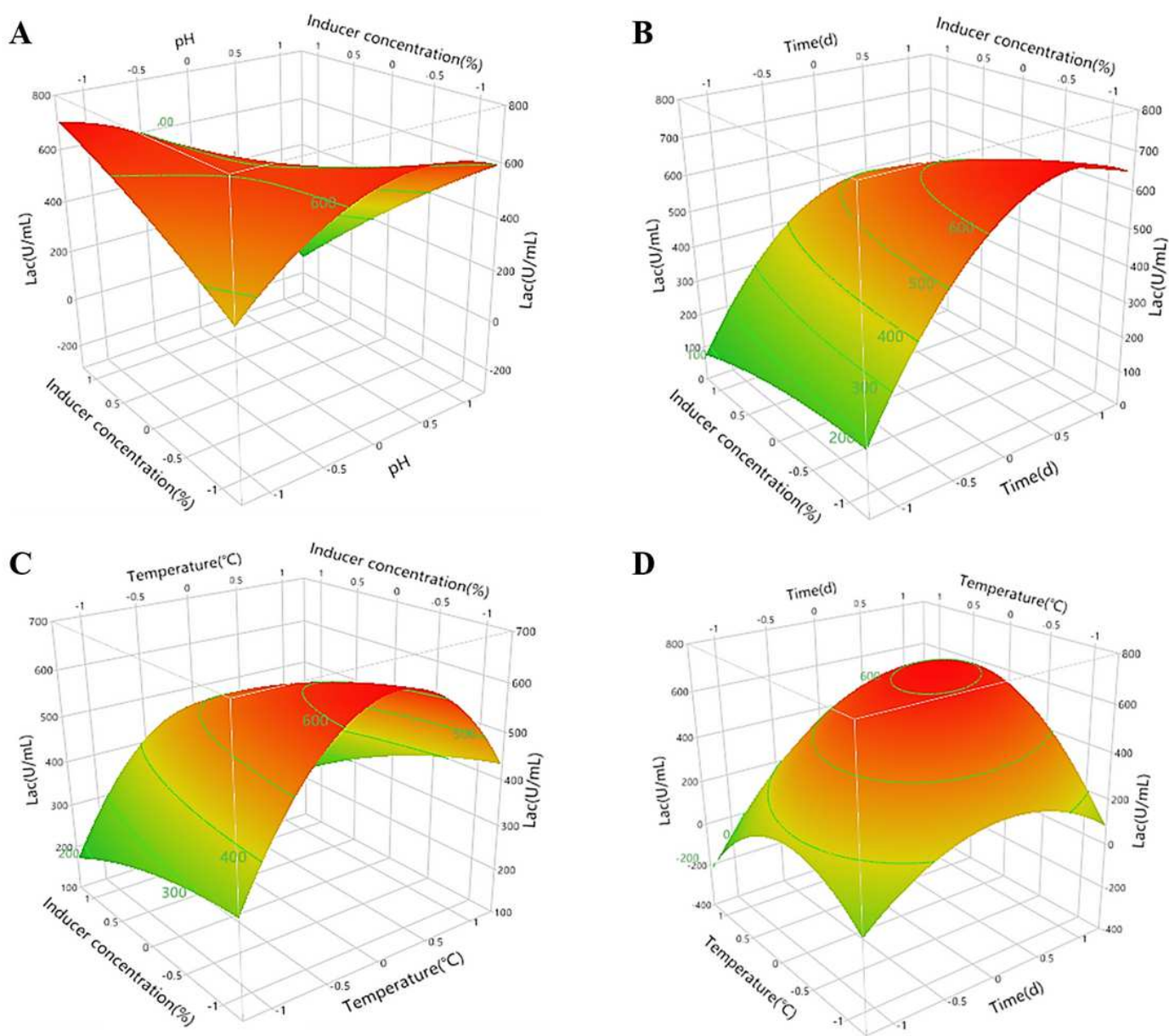


Figure 2

The influence of the interactions of two combinations of factors on laccase production in *Auricularia cornea*. (A) Interaction between inducer concentration and pH. (B) Interaction between inducer concentration and time. (C) Interaction between inducer concentration and temperature. (D) Interaction between temperature and time.

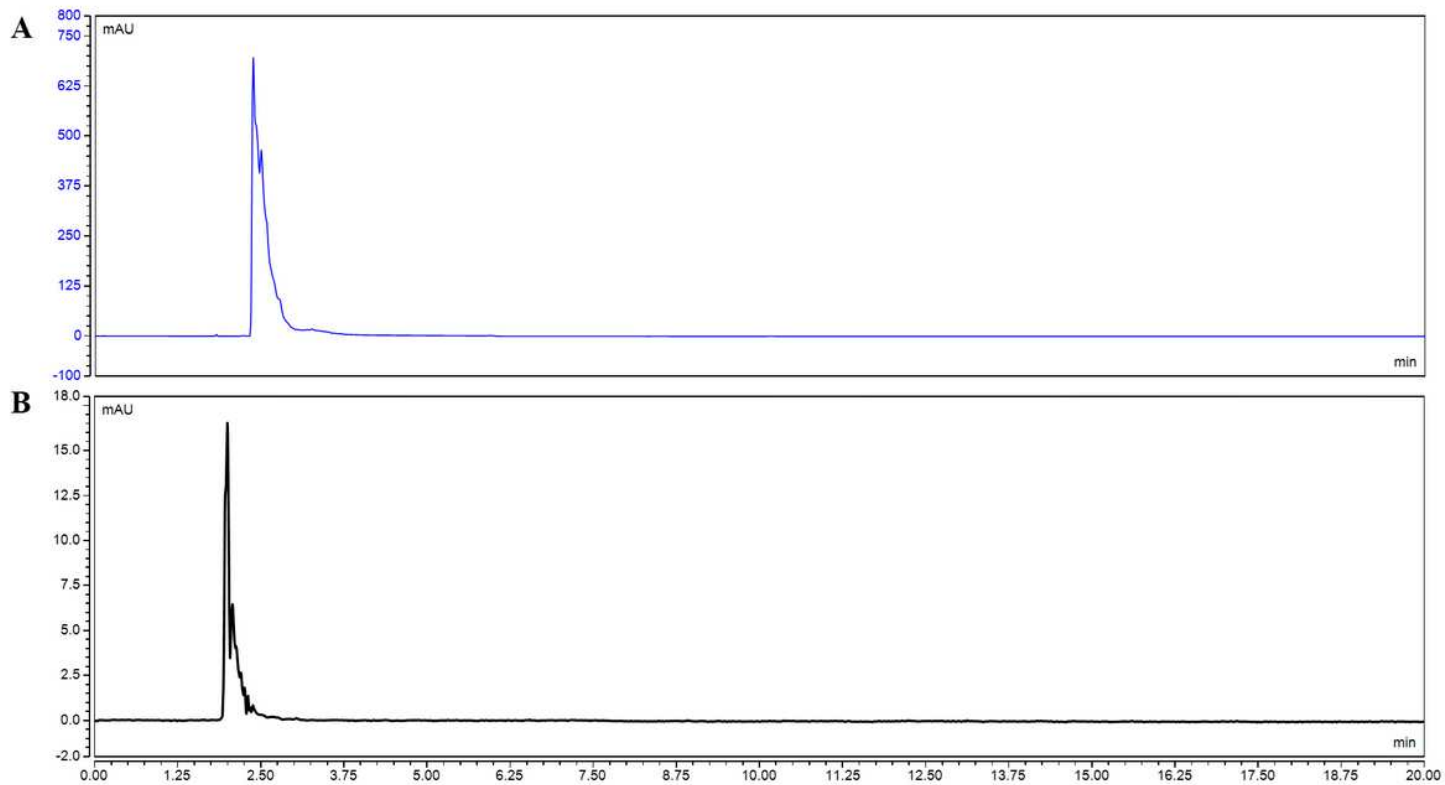


Figure 3

Decolorization analysis of malachite green dye by HPLC. (A) Original sample of malachite green dye. (B) Malachite green after degradation by *A. cornea* AC5 for 12 h.

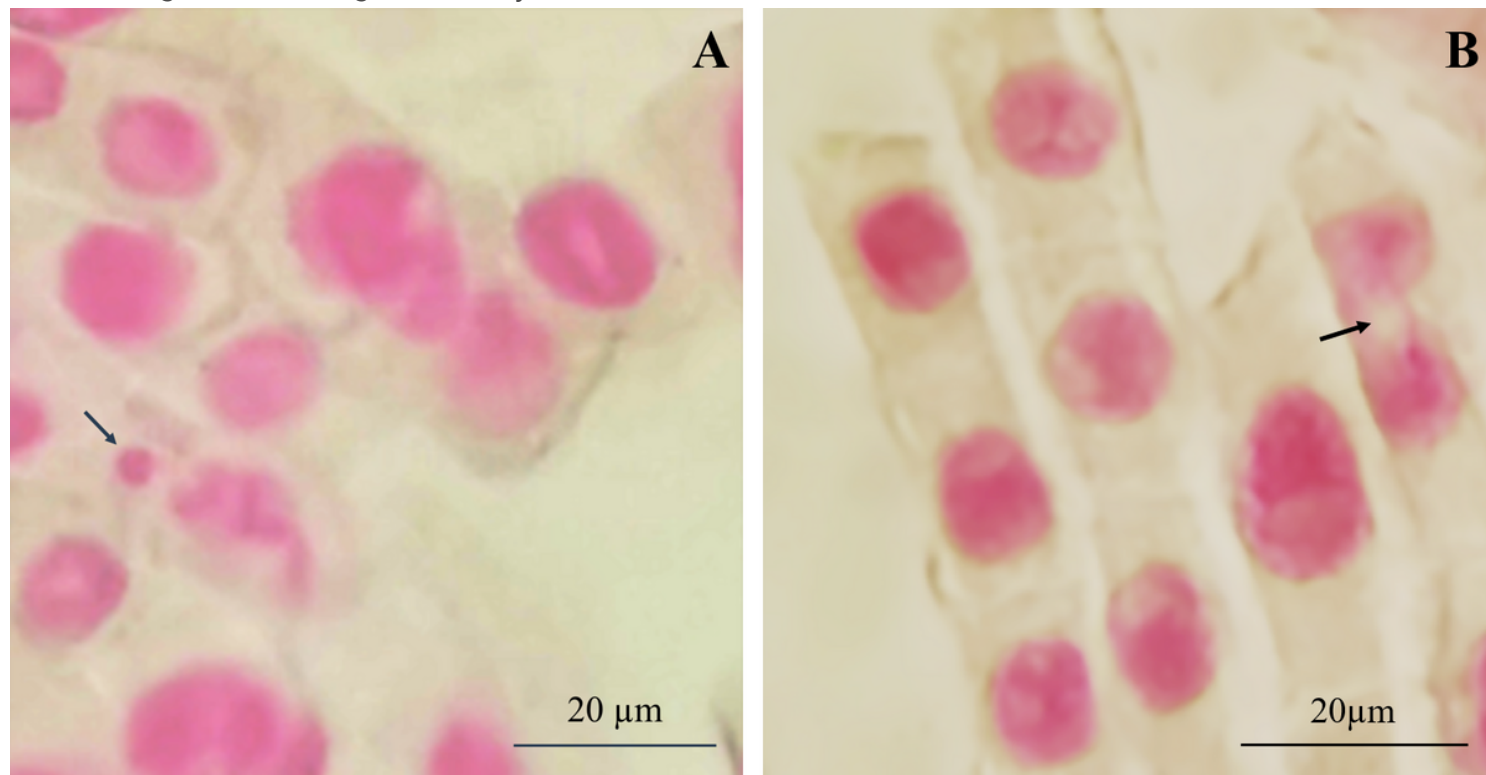


Figure 4

Cytotoxic damage induced in root meristematic cells of *Allium sativum* on treatment with malachite green. The black arrow in the picture refers to the chromosome variant cells. (A) micronucleus, (B) chromosome bridge.

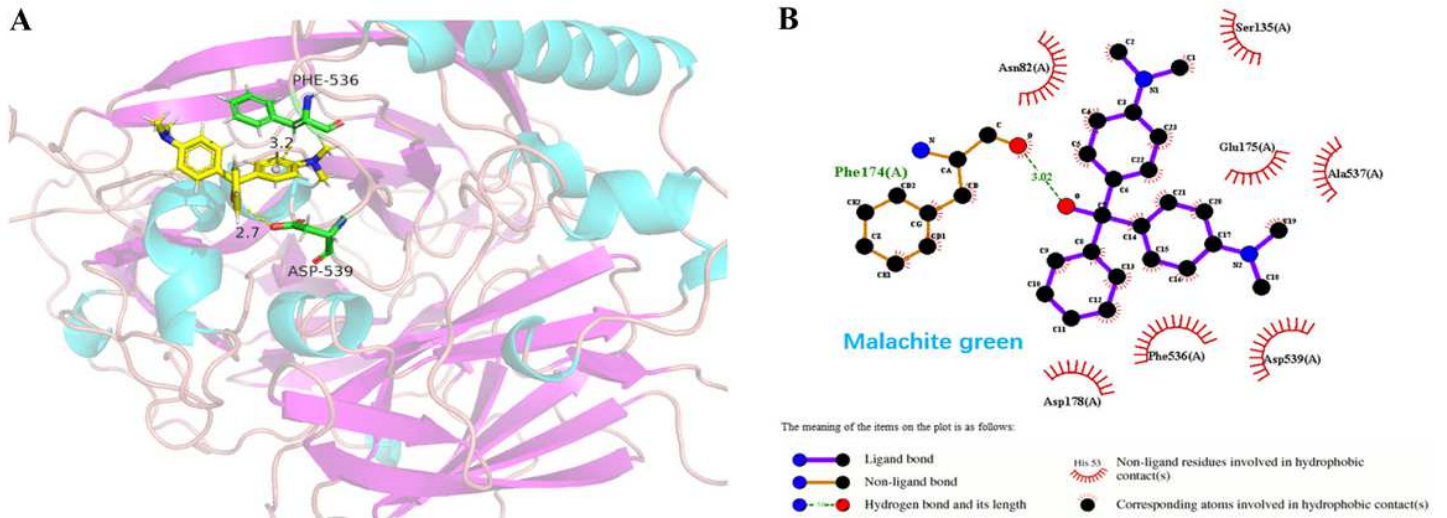


Figure 5

Structural model of molecular docking complex. (A) 3D model of molecular docking complex of laccase from *A. cornea* AC5 and Malachite green. (B) 2D ligand-receptor interaction diagram. Ligand interaction diagram indicating in detail how these residues interact with the ligand. Note the interactions between amino groups and acidic residues, specifically at Asn82, Ser135, Glu175, Ala537, Asp539, Phe536, and Asp178.